similar to those of group B, except that the CN bands are weak or absent. Later studies have shown that the type B and C stars have a substantial metal deficiency, around [Fe/H] = −1.4, whereas type A stars are less deficient, at [Fe/H] = −0.6 (Cardelli, 1989; Wahlgren, 1992). Given their very extended cool envelopes and possibly ongoing mass loss, RV Tauri photospheres may be deficient in the abundances of elements that easily condense into dust grains (Giridhar *et al.*, 2005).

Infrared excesses have indeed been observed for many RV Tauri stars, indicating the presence of circumstellar dust (Gehrz, 1972). Jura (1986) used IRAS observations to investigate circumstellar material around RV Tauri stars in the Galactic field, finding evidence that the mass loss rate of these stars has decreased, possibly by a factor of 100, during the past 500 years. Jura (1986) suggested that some of these stars might photoionize their circumstellar material as they moved to the blue in a post-AGB stage of evolution. Sloan *et al.* (2010) used infrared spectra obtained with the *Spitzer Space Telescope* to investigate mass loss and dust production in evolved globular cluster stars. There were four pulsating stars in their sample that straddled the dividing line between the longest-period W Virginis stars and RV Tauri variables. They did not find a dust excess for any of these stars, although they did find water-vapor emission in two of them.

8
Red Variable Stars

In this chapter, we discuss variability among red giant and red supergiant stars, located far to the low-temperature side of the H-R diagram in Figure 3.2. We saw in Chapter 1 that one of these variables, Mira (*o* Ceti), was the first pulsating star to have its period determined and that other Mira variables were also among the first periodic variable stars to be identified (Figure 8.1). Besides having low effective temperatures, these stars are distinguished by their deep convective envelopes, a circumstance important to understanding their behavior since the complicated process of convection has long posed challenges for theorists. Deep convection can mix the products of nucleosynthesis from the interior of a red giant to the surface. Molecules and dust grains can be formed in extended, cool atmospheres. Mass loss from the loosely attached atmospheres of red giants and supergiants can be significant. All in all, red giant variables test the mettle of theorists and observers alike.

It has long been known that variability is common among cool giant stars, with recent studies finding variability to be ubiquitous among stars in the red giant and asymptotic giant branch (AGB) stages of evolution. Jorissen *et al.* (1997) used Strömgren photometry to investigate variability at the several millimagnitude level in 50 red giant variables. They found that giants with spectral types from late G to early K were stable at the 6 millimagnitude level in the Strömgren *y* passband (which is close to Johnson's *V*; see Table 2.1), but that all of the giants with spectral types later than early K showed variability greater than that limit. Henry *et al.* (2000) obtained photometry of 187 red giants of spectral type G, K, and M0. About a third of these stars were found to be variable at >0.01 magnitudes in *V*. The proportion of variables was at a minimum for stars with late G spectral types, and increased both for early G stars and for those of K spectral type. All giants with spectral types of K5 and later were variable with amplitudes > 0.01 magnitudes. In fact, when photometry is pushed to very high accuracy, all red giants appear to be variable. Even the more stable yellow–orange giants of late G spectral type have been found to show solar-like *p*-mode oscillations that may be excited by turbulence in the outer envelopes of the stars (Frandsen *et al.*, 2002; Hekker, 2010; Stello *et al.*, 2013), as also discussed in Section 5.11.1. However, high-amplitude variability is generally reserved for AGB stars with high luminosities (Soszyński, Wood, & Udalski, 2013b).

Pulsating Stars, First Edition. Márcio Catelan and Horace A. Smith.

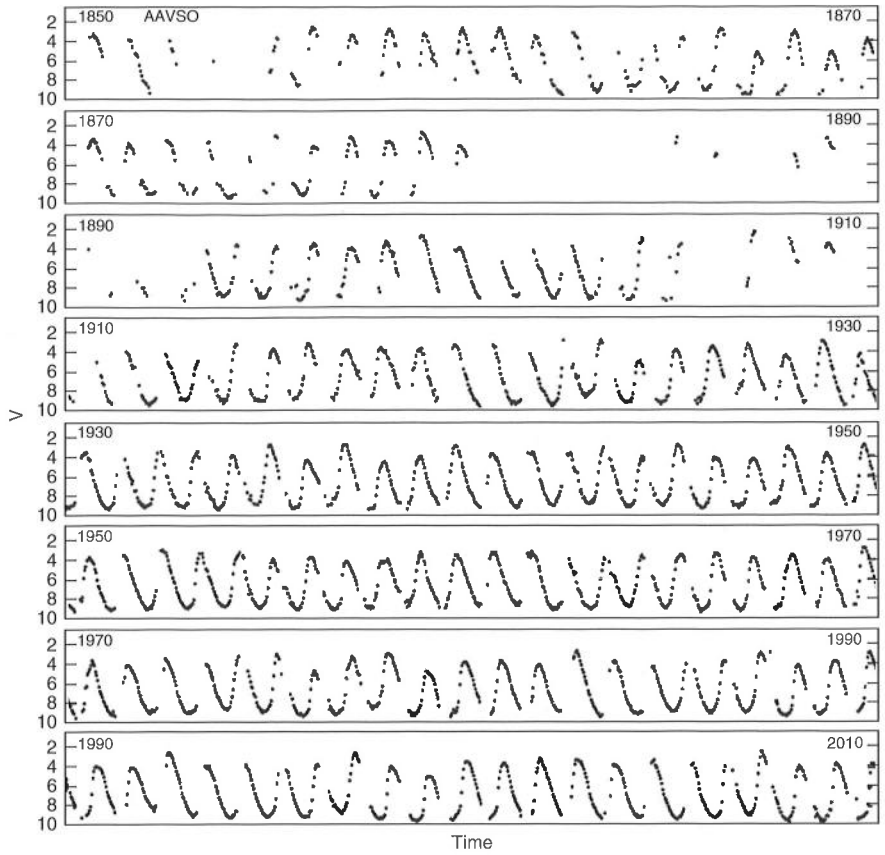

Figure 8.1 The AAVSO historical light curve of Mira, *o* Ceti, the first long-period variable to be discovered. (Based on data from Henden (2013). Courtesy AAVSO.)

There are a number of categories in the *General Catalogue of Variable Stars* into which pulsating red variables can be put. These include Mira variables, with visual amplitudes > 2.5 magnitudes and periods between 80 and 1000 days. In addition, there are variables of type SR (semi-regular red giants), SRa (semi-regular variables with persistent periodicity), SRb (semi-regulars with poorly defined periodicity), SRc (semi-regular variables that are red supergiant stars), SRd (semi-regulars that are orange to yellow supergiants), Lb (slow, irregular red giants), and Lc (slow, irregular red supergiants). Becker (1998) produced an H-R diagram similar to our Figure 3.2, but with the positions of red variables pertaining to these subdivisions schematically indicated as well. His plot, however, should be used only as a rough guide. Eggen (1977) also introduced a red variable classification system based upon visual amplitudes. In his scheme, large-amplitude red variables (LARVs) have visual amplitudes > 2.0 magnitudes, medium-amplitude red variables (MARVs) have V amplitudes between 0.5 and 2.0 magnitudes, and small-amplitude red variables (SARVs) have V amplitudes

smaller than 0.5 magnitudes. SARVs discovered in the OGLE survey have been termed *OSARG stars*, standing for OGLE Small-Amplitude Red Giants (Wray, Eyer, & Paczyński, 2004). These variables have amplitudes smaller than about 0.13 magnitudes in the Cousins I band. Soszyński *et al.* (2009b) note that traditionally variables within their OSARG class would either not have been discovered at all or, if found, would have been included in the class of SR variables.

All of these variables, except perhaps some of the SRd variety, are either red giant or red supergiant stars. They have large radii, tens or hundreds of times the radius of the Sun, and correspondingly low mean densities. Ritter's relation (Equation 5.22) leads us to expect that these variables will have long periods. That is indeed the case, and Mira and related SR variables are often grouped into the general category of *long-period variables* (LPVs).

Clement *et al.* (2001) listed 120 red giant variables in their catalog of variable stars within globular clusters. However, many more such stars are known outside of globular clusters. Soszyński *et al.* (2009b) identified 91 995 red giant variables in the Large Magellanic Cloud, including 1667 Mira-type variables, 11128 SR variables, and 79 200 OSARG variables. Toward the Galactic bulge, the OGLE project has identified 232 406 long-period variables, including 6528 Mira stars, 33 235 SR variables, and 192 643 OSARG stars (Soszyński *et al.*, 2013a).

Red giant and supergiant variables have spectral types appropriate for cool stars: late K, M, S, or C (see Figure 3.2). Stars of M, S, and C spectral type overlap in effective temperature but differ in the chemistry of their atmospheres. S-type spectra have zirconium oxide bands and may have enhanced *s*-process elements. This zirconium oxide absorption is not seen in the spectra of ordinary M-type stars. C-type classifications are used for carbon stars, but the earlier R and N classifications for carbon-rich stars can sometimes still be encountered (Giridhar, 2010). Merrill (1940) wrote an important monograph on the spectra of long-period variables, but his study is mainly concerned with the blue region of the spectrum to which the photographic plates of the day were more sensitive. More recently, spectroscopy of long-period variables has been extended further to the red, nearer the peak in the energy distributions of these stars (Castelaz *et al.*, 2000; Lançon & Wood, 2000).

8.1 Convection and Pulsation

Before considering further the properties of red variables, it is necessary to write a few words about the effects that convection can have on pulsation. The interplay of pulsation and convection has already been discussed in Chapter 5. There we saw that convection played an important role in quenching pulsation at the red edge of the instability strip inhabited by Cepheids and RR Lyrae stars (Section 5.10). The red giant and supergiant variables discussed here lie well beyond the cool edge of that strip. The dominant means of energy transport in the outer envelopes of these stars is convection rather than radiation. This would lead us to expect

that the κ mechanism, which works by modulating radiative energy transport, would in general not be an efficient driving mechanism for pulsation in red giants. Moreover, as we have already seen in Section 5.10.1.3, there are alternative ways in which pulsation can be excited in these stars, for example, by convection-driven turbulence. Since Mira variables do indeed pulsate, a correct understanding of the interaction between pulsation and convection must provide a mechanism, or combination of mechanisms, that allows pulsation to occur. However, our incomplete understanding of processes associated with convection has made finding the correct mechanism a challenging endeavor.

At the foot of the red giants variables in Figure 3.2 we encounter the *ξ Hydrae variables*, thus named after the prototype of the class of red giant pulsators undergoing solar-like oscillations (Frandsen *et al.*, 2002; Houdek & Gough, 2002). The study of pulsations in these very low-amplitude stars depends to a large degree on space-based observations with *MOST*, CoRoT, and *Kepler*. Variables of this type fall into the realm of the stochastically excited variables discussed in Section 5.10.1.3, and turbulent convection is believed to play a dominant role in exciting their oscillations. We will not discuss these solar-like oscillators in this chapter, but refer the reader to the references in that section and to Hekker & Mazumdar (2014).

Above the ξ Hydrae variables in Figure 3.2, we find long-period variables, including Mira stars and SR red giant variables. Early linear and nonlinear pulsation models of these stars (Keeley, 1970; Wood, 1974; Fox & Wood, 1982; Ostlie & Cox, 1986; Cox & Ostlie, 1993) had some success, but the details of the excitation mechanism, identifying the correct pulsation mode, and properly accounting for the interaction of pulsation with convection all proved to be difficult problems. For example, the usual mixing length theory of convective energy transport, often employed in modeling static stars, is inadequate for these pulsating stars (Ostlie & Cox, 1986). Early models indicated that the hydrogen ionization zone near 10 000 K (see Figure 5.15) plays an important role in exciting the pulsation of long-period variables. However, there were indications that driving from the hydrogen ionization zone was not the whole story and that convection itself might destabilize giant stars at low effective temperatures, especially when the convective timescale is shorter than the dynamical timescale.

Recent models have attempted to shed more light on how pulsation occurs in a star with a convective envelope. Munteanu *et al.* (2005) constructed one-zone models with a time-dependent convective term to explore the coupling between pulsation and convection, investigating whether pulsation in long-period variables might be driven by a convection-related process or by the κ and γ mechanisms. In their modeling, they found that the strong convection led to the disappearance of the κ mechanism, with the driving being supplied only by the γ mechanism. Their calculations further suggested that convective processes, rather than the γ mechanism, were most important, and that turbulent pressure could be a driving mechanism for pulsation. Nonlinear pulsation models by Olivier & Wood (2005) included prescriptions for time-dependent convection, turbulent pressure, and turbulent viscosity. Their models suggested that turbulent pressure and turbulent

energy transport might have only a small effect on many basic pulsation properties but that inclusion of turbulent viscosity might be needed to decrease modeled pulsation amplitudes so that they better match those observed. Models by Xiong, Deng, & Cheng (1998) and Xiong & Deng (2007, 2013) provided additional support for the idea that convection in red giants can serve to drive as well as quench pulsation. In their models, it is the coupling between convection and the oscillations of the red giant stars that replaces the classical κ mechanism as the driver, allowing the existence of a red giant "instability strip" at lower effective temperatures than the Cepheid instability strip. These are very interesting results, but it is too soon to say that we have a good grasp of all of the ways in which convection and pulsation interact.

8.2 Mira and Related Long-Period Variables

As noted above, Mira variables have pulsation periods from 80 to 1000 days and visual amplitudes > 2.5 magnitudes. In some stars, the visual amplitude can be as high as 8 magnitudes, corresponding to a factor of more than a thousand in visible light flux. The bolometric amplitude is much smaller, about 1 magnitude, as discussed further below. We saw in Chapter 1 that several examples of this common type of variable star were among the first variable stars to be discovered, thanks to their large amplitudes and the relatively bright apparent magnitudes of several nearby Mira variables (see Table 1.1). Figure 8.2 shows a portion of the visible light curve of the Mira variable χ Cygni.

Mira variables are giant stars with effective temperatures near 3000 K. They are believed to be nearing the tip of the AGB. They are thus cool giant stars with very large radii, powered by fusion from both a hydrogen-burning shell and a

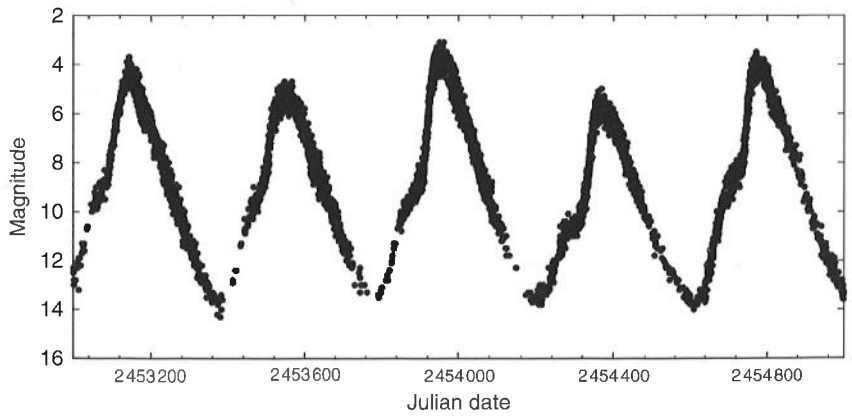

Figure 8.2 This figure shows the visual light curve of the 408-day-period Mira variable χ Cygni. (Based upon observations from the AAVSO International Database (Henden, 2013). Courtesy AAVSO.)

helium-burning shell, as discussed in Chapter 4. With radii that can reach a few hundred solar units, Mira stars have very low average densities, as noted in Section 5.2. As a star climbs toward the tip of the AGB its radius increases while its mass either stays constant or, more likely, diminishes through mass loss, resulting in a further decline in its already low mean density.

Mass loss is very important for understanding the evolution and properties of AGB stars, and this is discussed further below. However, it is useful to note here that Mira variables may have experienced mass loss even before arriving at the AGB (Section 4.2). During the Mira stage itself, it appears that the stars are in the process of undergoing significant mass loss. Mira variables are thus less massive than they were when they were at the main-sequence (MS) turnoff. How much mass has been lost is, however, not a quantity for which we can make good theoretical calculations.

The oldest Mira variables (such as those seen in globular clusters) are believed to have masses near 0.6 $M_\odot$. However, some Mira variables are younger and can be found in intermediate-age stellar populations. The most massive Mira variables may have main-sequence progenitors with masses as great as 4–6 $M_\odot$, as noted in Section 4.4. A number near 1 $M_\odot$ is often used to describe the mass of a typical Mira variable. In the Milky Way, the shortest-period Mira variables also have the lowest masses and metallicities (Feast & Whitelock, 2000; Willson & Marengo, 2012).

Mira variables therefore can have progenitors of either low or intermediate mass. At the low-mass limit, Miras are as old as the globular clusters, about 10^{10} years. However, Mira variables with intermediate-mass progenitors can be as young as a few $\times 10^8$ years. Note that the highest-mass progenitors of Mira variables have masses greater than the upper limit for stars that undergo the helium-core flash (see Section 4.2). Helium burning in such stars will begin in a nondegenerate core (Section 4.3).

Mira variables can be divided into oxygen-rich and carbon-rich varieties, depending on whether their photospheric C/O abundance ratios are less than or greater than 1, respectively. Most Miras belong to the oxygen-rich variety. However, as noted in Section 4.3, AGB stars can dredge up material from deep within, changing their surface chemical compositions. Carbon-rich Mira variables can be created by this dredging process. *Spitzer Space Telescope* observations of evolved stars in the Magellanic Clouds indicate that carbon-rich stars are more likely to be produced in a low metal abundance population than in one of high metallicity (Blum *et al.*, 2006; Boyer *et al.*, 2012; Willson & Marengo, 2012). The unusual atmospheric abundances of variables of spectral type S are also attributed to the dredge up of processed material from the deep interior. The discovery of lines of a relatively short-lived radioactive isotope of technetium in stars with S-type spectra, including long-period variables (Merrill, 1952), provided clear evidence of an element that could only have been produced relatively recently in the interior of those stars and brought to the surface in the third dredge up.

Mira variables are believed to be pulsating in a radial mode, but for a long time it was debated whether they pulsated in the fundamental or the first-overtone mode.

Determining the pulsation mode is in principle straightforward if one has the right information. If you know the radius and mass of a Mira star, measure its period, and have a good theoretical knowledge of the pulsation constant, Q, for particular pulsation modes, then Ritter's relation (Section 5.2) allows you to determine in which mode the star pulsates. The major problem with applying this method was the uncertainty as to what the radii of Mira variables actually were.

Good parallaxes are known for a number of Mira variables, for example, from the Hipparcos mission (van Leeuwen *et al.*, 1997) or from VLBI observations of OH masers in the extended atmospheres surrounding Mira variables (Kurayama, Kobayashi, & Sasao, 2005). If the angular diameter of these stars is also known, for example from interferometry, the physical diameter of the star can be calculated. Pease (1931) was long ago able to resolve Mira itself using a Michelson interferometer on the 2.5-m Mount Wilson telescope, and angular diameters have now been measured for several such variables. At first, diameters from interferometry of Mira variables suggested that the first-overtone mode might be the correct pulsation mode (Tuthill *et al.*, 1994). However, it was later found that these studies gave too large an angular diameter because they were biased by the existence of cool molecular layers above the actual surface of the Mira variables (Perrin *et al.*, 2004). Later interferometric studies yielded smaller values for the diameter of the actual stellar surface, and there is now consensus that Mira variables pulsate in the fundamental mode.

Observations of the numerous red variables in the Large Magellanic Cloud have proved important to understanding their period–luminosity relations. Wood *et al.* (1999), using observations from the MACHO project, identified several roughly parallel period–luminosity relations for long-period variables in the Large Cloud, assigning a letter designation to each. Later work has confirmed and expanded on this discovery (Ita *et al.*, 2004; Soszyński *et al.*, 2009b). In Figure 8.3 we present a recent version of this diagram, which is also known as the *Wood diagram*, named after Peter R. Wood.

Figure 8.3 plots a reddening-independent Wesenheit index against period for long-period variables found in the OGLE survey of the Large Magellanic Cloud. In this case, the Wesenheit index is calculated from near-infrared observations in J and K, drawn from the 2MASS survey: $W_{JK} = K - 0.686\,(J - K)$. Colors indicate the amplitudes of variability in the Cousins I band. Sequences are identified by letter and the gray line indicates a fit to the points in sequence C′. Use of near-infrared photometry, as well as adoption of the Wesenheit index, minimizes the effects of extinction due to dust. This is particularly important because Mira variables can be surrounded by interstellar dust shells. Carbon-rich and oxygen-rich Mira variables also seem to follow the same period–luminosity sequence in the JK Wesenheit index-period diagram, whereas carbon-rich and oxygen-rich Miras appear to occupy somewhat different sequences if the VI-band Wesenheit index is used instead (Soszyński *et al.*, 2005, 2007).

In Figure 8.3 we can see that the highest-amplitude variables lie along sequence C. Sequence C includes the Mira variables, which are now believed to be pulsating in the fundamental radial mode, but it also includes some of the SR variables.

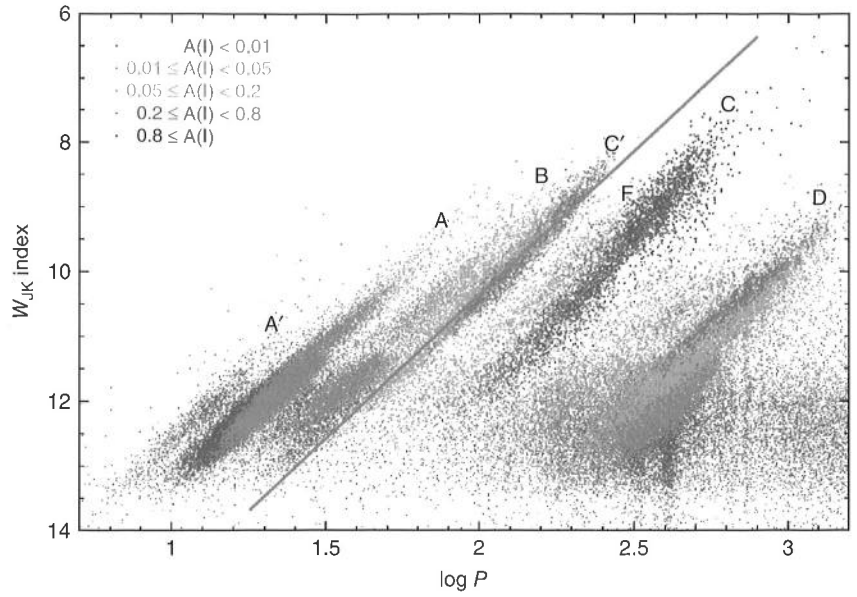

Figure 8.3 Period–luminosity relations (Wood diagram) for red giant variables in the Large Magellanic Cloud. Different colors indicate the *I*-band amplitude, while the letters denote ridges followed by different families of variables (Miras follow ridge C; OSARGs follow A, A′, C; SRs follow C, C′, F; binaries follow E; and D remains unexplained). (Based on data from the 2MASS and OGLE surveys. From Soszyński, Wood, & Udalski (2013b). Copyright American Astronomical Society.) (Please find a color version of this figure on the color plates.)

We shall see in Section 8.3 that other sequences include SR and OSARG variables, some of which are pulsating in multiple modes. Soszyński, Wood, & Udalski (2013b) argue that OSARG stars, SR red variables, and Mira variables form a continuous sequence. In their interpretation, as a red giant evolves it changes from an OSARG variable to an SR variable and then to a Mira variable. As it does so, its amplitude increases and the number of pulsation modes that are excited decreases. The existence of a period–luminosity relation for Mira variables (albeit with some scatter) means that, as with the Cepheids, they can be used as standard candles for determining distances.

The small bolometric amplitudes of Mira variables were first demonstrated by Pettit & Nicholson (1933). They used a thermocouple at the Newtonian focus of the Mount Wilson 2.5-m telescope to measure the energy received from 11 long-period variables. They concluded that the luminosities of such variables varied by about a factor of two during the pulsation cycle, and that the surface temperature varied by about 30%. Recent measures of the bolometric amplitudes of Mira variables are consistent with this pioneering result. These low-temperature stars emit most of their energy in the infrared, and their amplitudes in long-wavelength photometric bandpasses, such as the 2.2-micron *K* band, are small compared to their visual amplitudes, typically about 1 magnitude. This is illustrated in Figure 8.4,

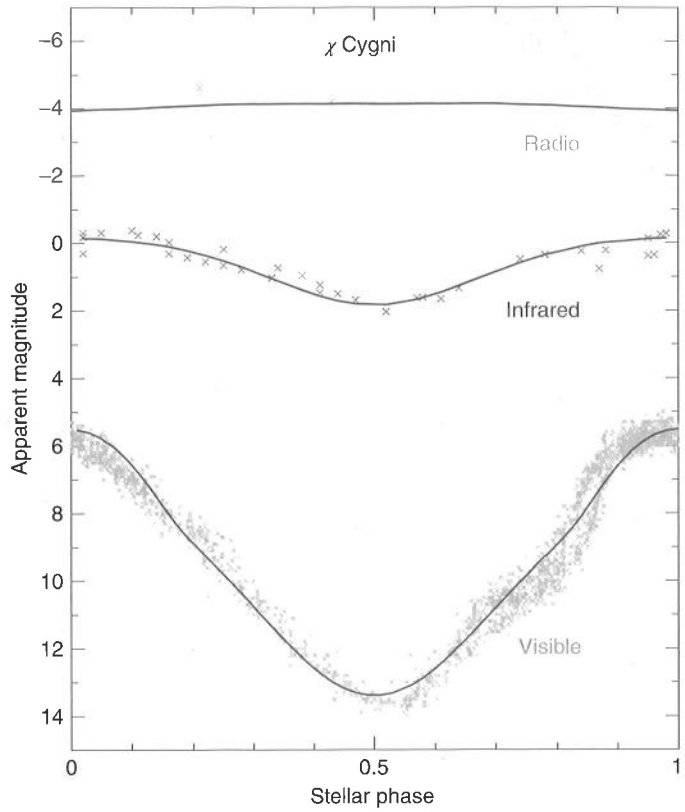

Figure 8.4 Radio (3.6 cm), infrared (1.04 microns), and visible light curves of χ Cygni. In this figure, the lines are not fits to the data, but represent the predictions for an oxygen-rich Mira with an extended atmosphere. (From Reid & Goldston (2002). Copyright American Astronomical Society.)

where the radio, infrared, and visible light curves of the Mira variable χ Cygni are compared.

Since the visual portion of the Mira spectrum is on the short-wavelength tail of the spectral energy distribution, we might readily imagine that the visual magnitude will change more than that in the infrared as the stellar temperature changes during the pulsation cycle. However, the changes in visual amplitude expected from changes in effective temperature and radius are smaller than those often observed, which can be as large as 6–8 magnitudes. The reasons for this discrepancy were explored by Reid & Goldston (2002). They noted that one cannot simply explain the emission from a Mira variable by assuming blackbody thermal emission from a star that changes radius and effective temperature as it pulsates.

Reid & Goldston (2002) noted that, at maximum brightness, a Mira variable is smaller and hotter than at minimum. During maximum, the extended atmosphere of the Mira is more transparent to visible light, allowing the observer to see more deeply into the star to a region of higher temperature. As the star expands and

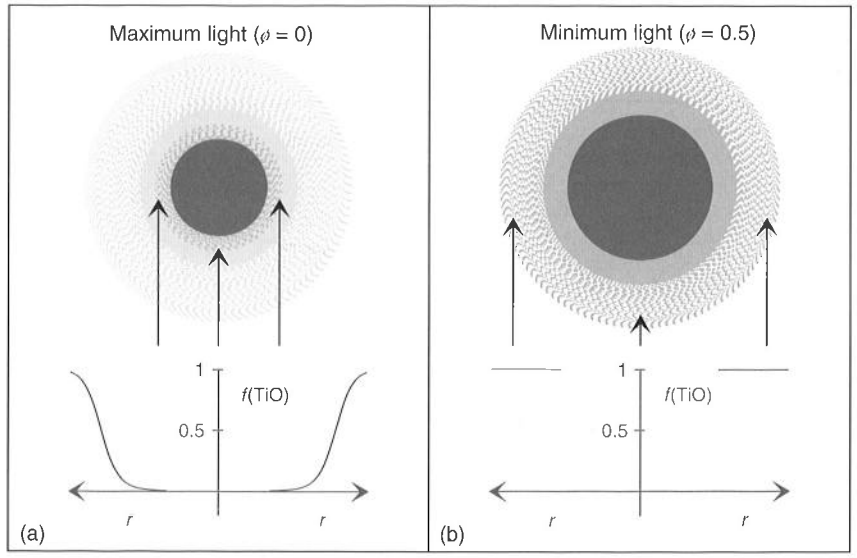

Figure 8.5 Schematic diagram of Mira at maximum (*left*) and minimum (*right*) brightness. The "star" itself is shown in dark gray. The extended very low-density atmosphere surrounding it is shown in lighter gray. Arrows show the depths to which visible light observers can see. The fraction of Ti in the form of TiO is shown by f(TiO). Near minimum, absorption from TiO prevents the visible light observer from seeing nearer than about 1.8 times the radius of the star, whereas infrared observations penetrate more deeply. (From Reid & Goldston (2002). Copyright American Astronomical Society.)

cools during the decline to minimum, metallic oxide molecules, such as titanium oxide (TiO), form within an extended atmosphere. These oxides make the atmosphere more opaque to visible light. At visual wavelengths, the observer sees to a shallower depth in the atmosphere and the visual photosphere at minimum can be twice as large as at maximum light, with a temperature that can fall to 1400 K. The net result is that little light emerges at visible wavelengths near minimum light compared to maximum light. This is illustrated in Figure 8.5. By contrast, the molecular opacity is low at infrared wavelengths. At minimum light the infrared observer sees more deeply into the star than does the visual observer. There is still a change in infrared emission as the Mira star warms and cools, expands and contracts, during pulsation, but the difference is much smaller in the infrared than in the visual. Because of the changes in molecular absorption during the light cycle, the usual $B-V$ and $U-B$ color indices are of little use in determining the change in effective temperature of a Mira variable.

In carbon-rich Mira variables, the situation is somewhat different. Reid & Goldston (2002) noted that essentially all of their atmospheric oxygen is bound into CO, preventing the abundant formation of TiO or other oxides. Smaller visual amplitudes might be expected for such stars (Willson & Templeton, 2009). However, Reid & Goldston (2002) proposed that carbon-bearing molecules probably play some role in the visible amplitudes of carbon-rich Miras. They also suggested

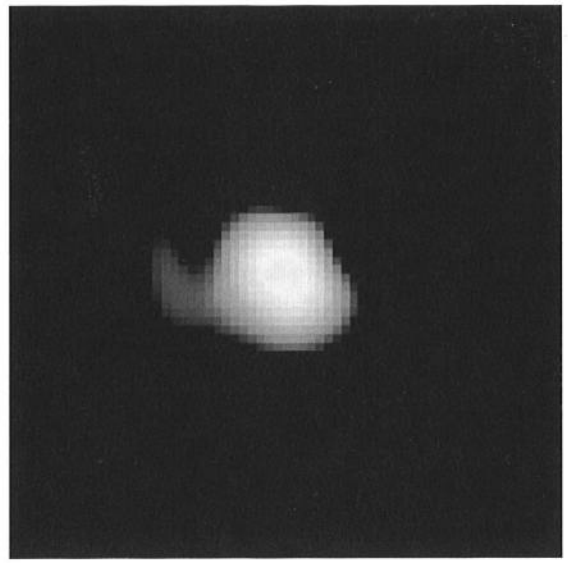

Figure 8.6 Resolved ultraviolet image of Mira, obtained with the *Hubble Space Telescope*. The image shows a hook-like appendage extending from Mira in the direction of its companion. (From Karovska *et al.* (1997) and Karovska (1999); see also NASA and STScI Press Release STScI-PRC97-26, 1997.)

that the formation of dust shells at distances > 3 stellar radii might contribute to the dimming of optical light in both carbon-rich and oxygen-rich Miras.

We should emphasize that differences in opacity at different wavelengths mean that different stellar radii are observed at different wavelengths. Angular radii of Mira variables have been measured using lunar occultations (Baug & Chandrasekhar, 2012), interferometry (Mennesson *et al.*, 2002; Perrin *et al.*, 2004; Ragland *et al.*, 2006; Lacour *et al.*, 2009; Karovicova *et al.*, 2011), surface brightness methods such as the Barnes–Evans method (Barnes & Evans, 1976), and, in a few cases, by direct imaging (Karovska, 1999). When sufficient resolution of a Mira variable was achieved the resultant image has often not been completely spherically symmetric. This can be seen, for example, in *Hubble Space Telescope* images of Mira itself (Figure 8.6; see Karovska *et al.*, 1997; Karovska, 1999) and in infrared observations of χ Cygni with the IOTA interferometer (Lacour *et al.*, 2009). χ Cygni showed a 40% change in radius during the pulsation cycle, as well as limb darkening and inhomogeneities in the stellar disk that changed with time.

In Chapter 1, we noted that the presence of emission lines in the spectrum of a star of spectral type M was an early indicator that the star might be a long-period variable. This emission is indicative of shock waves in the atmospheres of Mira variables. Bowen (1990) and Willson (2000) have argued that shock waves can "levitate" the atmosphere of a Mira variable. The result is that the outer atmosphere of a Mira is denser than it would be for the corresponding static atmosphere, making it easier for the Mira to lose mass. Dust grains that form in this extended

cool atmosphere can be pushed outward by radiation, promoting mass loss as they also drag away surrounding gas. Mass loss may be largest near the tip of the AGB, where not only is the star brightest, but also the extended atmospheres of Mira variables are very loosely held. As the Mira evolves up the AGB, its radius expands and its period would be expected to increase. Thus, mass loss may be expected to be larger for longer-period Mira variables, all else being equal.

Mass loss is indeed large and important among Mira variables. Mira itself, a member of a binary star system, provides dramatic evidence for mass loss. Ultraviolet observations of Mira reveal a tail extending two degrees to the north along with an arc-like feature to the south (Martin *et al.*, 2007). Martin *et al.* suggested that the arc-like feature indicates the existence of a bow shock, as mass loss from Mira encounters the interstellar medium. They interpret the extended tail as the result of ram-pressure stripping of material as Mira moves through the interstellar medium. From the speed of Mira's motion through the interstellar medium, Martin *et al.* calculated that the tail of the stripped material was about 30 000 years old. However, Wareing *et al.* (2007) suggested that the tail might be much older, perhaps as old as 450 000 years. Further simulations of Mira's tail have been carried out by Esquivel *et al.* (2010) and Gómez (2013). Figure 8.7 shows Mira as seen in ultraviolet, infrared, and X-ray wavelengths. In Figure 8.7a, *GALEX* ultraviolet observations reveal the extended tail mentioned above, which can also be appreciated in the cover of this book. In Figure 8.7b, infrared observations obtained at 70 microns with the Herschel telescope (Mayer *et al.*, 2011) show extensive material ejected from Mira. In Figure 8.7c, X-ray observations with the *Chandra* spacecraft show Mira and its companion star (Karovska, 2006). The connection between the

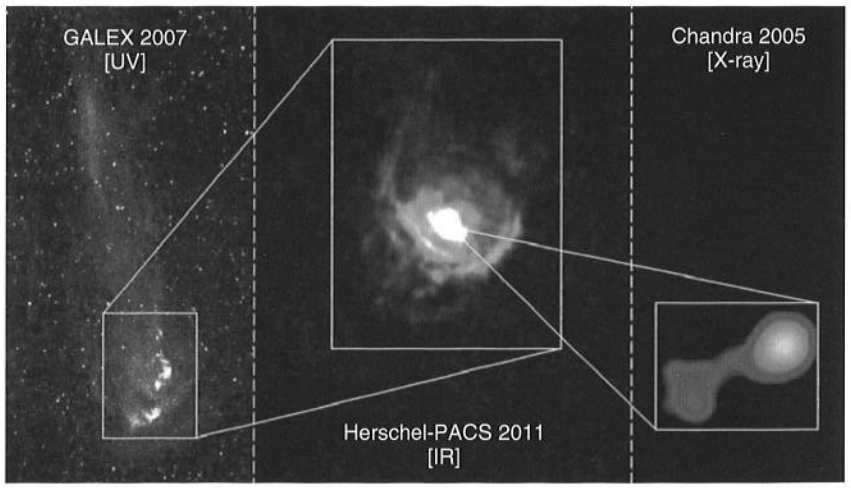

Figure 8.7 Ultraviolet (a), infrared (b), and X-ray (c) observations of Mira reveal evidence of ongoing mass loss. (Institut d'Astronomie et d'Astrophysique, Université Libre de Bruxelles, press release: http://www.astro.ulb.ac.be/pmwiki/IAA/Press. Courtesy ESA and NASA.)

two components in Figure 8.7c suggests possible mass flow from the variable to its hotter companion.

In addition to Mira itself, other Mira variables are known to be surrounded by extensive shells of gas and dust. Uttenthaler (2013) found a correlation between the mass-loss rate of a Mira variable and its period, with increased mass loss correlating with longer periods. There were actually two distinct relations, one for Mira variables that showed technetium in their spectra and one for those that did not. The technetium-poor Miras had higher mass loss rates than their technetium-rich counterparts. Sloan *et al.* (2010) used *Spitzer Space Telescope* infrared spectra to investigate circumstellar material around 35 long-period variables in globular clusters. While some of these variables did not show circumstellar dust excesses, many showed emission from oxygen-rich dust and one showed emission from carbon-rich dust. Stars with lower metallicities tended to be surrounded by less dust, but they did not find a trend with pulsation period.

Ita & Matsunaga (2011) used the near- to mid-infrared period–luminosity relations for Mira variables in the Large Magellanic Cloud to investigate the dimming of Miras by circumstellar dust. Dusty Miras were fainter than expected on the basis of the period–luminosity relations, with the amount of deviation being strongly correlated with the near-infrared colors of the variables. Moreover, the infrared observations indicated that the properties of the dust surrounding a Mira are correlated with the period of the Mira, implying that the circumstellar dust changes as a Mira variable evolves up the AGB. New results for Miras and other variables in the Magellanic Clouds are expected soon in the infrared from the IRSF/SIRIUS survey (Ita & IRSF/SIRIUS Variable Star Survey Team, 2009).

What happens to Mira variables after they leave the AGB? Presumably, most eventually find their way to the white dwarf cooling sequence, as expected for most low- and intermediate-mass stars (Chapter 4). Whitelock & Feast (1993) found that the data were consistent with the idea that, on their way to becoming white dwarfs, most Mira variables first evolve into planetary nebulae. That seems less likely now. Willson & Marengo (2012) point out that there are only about 15% as many planetary nebulae produced each year as there are stars that leave the AGB. From that, they conclude that few, if any, Mira variables end up as planetary nebulae. Willson & Templeton (2009) also suggest that low-mass, low-luminosity, and low- metallicity Mira variables could become RV Tauri stars, close to the end of their careers as red giants.

Although the brightest Mira variables were among the first pulsating stars to be discovered, the observational histories of even these bright Mira variables often have significant gaps until the latter part of the nineteenth century. Because of their long periods, we frequently have observational records extending over fewer than 150 cycles, even for those Mira variables that can be counted as well observed. Although the light curves of Mira variables are not so irregular as to place them in the category of SR variables, their light curves do not repeat precisely from one cycle to the next, as shown in Figure 8.2.

Averaging light curves over several cycles reveals that the mean visual light curves of Mira variables differ from star to star. Different classification schemes

have been advanced to describe and classify these different light curve shapes (Ludendorff, 1928; Campbell, 1955; Mennessier, 1985; Vardya, 1988). Melikian (1999) proposed a relatively simple classification scheme for the Mira variables observed by the Hipparcos satellite, dividing the stars into those with sinusoidal light curves and those with more complex light curve shapes. It is possible that supergranular convection in the envelopes of Mira variables is one contributor to the noise in their light curves (Templeton & Karovska, 2009).

Early studies of period changes of Mira variables (Eddington & Plakidis, 1929; Sterne & Campbell, 1937) attempted to distinguish significant period changes from random cycle-to-cycle period fluctuations using as a tool $O-C$ diagrams (Section 2.3) for the time of maximum light, an approach also adopted in some more recent investigations (Percy & Colivas, 1999; Percy & Au, 1999). Karlsson (2013) compiled dates of maximum and $O-C$ diagrams for 489 Mira variables.

Templeton, Mattei, & Willson (2005) used wavelet analysis to investigate the period changes of 547 Mira variables having extensive observations in the AAVSO International Database. The average period of these Mira stars is 307 days. 57 stars, 21 stars, and 8 stars had values of $d \ln \mathcal{P}/dt$ that were significant at the 2σ, 3σ, and 6σ levels, respectively, where $\mathcal{P}$ is the period. The eight Mira variables with the most significant period changes have also been identified in other period change studies. Figure 8.8 (courtesy of M. Templeton 2013, private communication) shows period versus time for T UMi, one of those rare Mira variables with a dramatically changing period. The period behaviors of the eight stars with large period changes are not, however, identical, and both period increases and period decreases have been observed.

It has been argued (Wood & Cahn, 1977; Wood & Zarro, 1981; Templeton *et al.*, 2005) that Mira variables undergoing large period changes are AGB

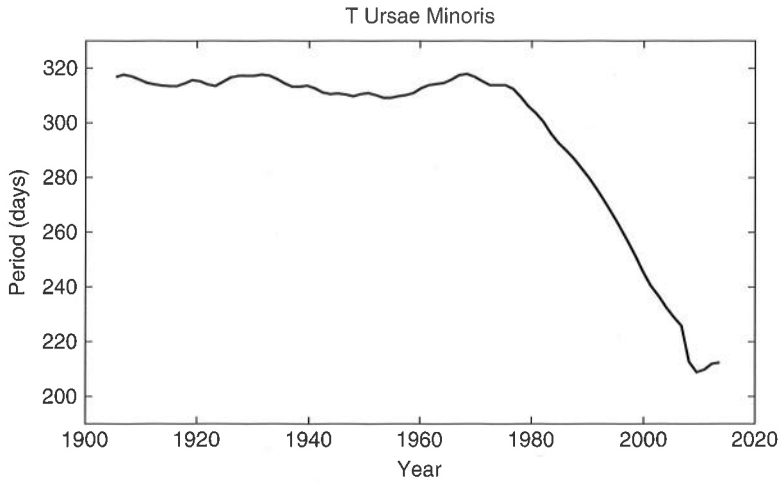

Figure 8.8 This figure, an update of Figure 8 in Templeton *et al.* (2005), shows the large decrease in the pulsation period of the Mira variable T UMi that may be associated with a thermal pulse. (Based on AAVSO data. Courtesy M. Templeton.)

stars undergoing thermal pulses (see Section 4.2). The 1.6% of Miras in the Templeton *et al.* (2005) sample with large period changes is consistent with the 1 or 2% expected to be experiencing thermal pulses during a shell flash event (see Chapter 4). It is not certain, however, that all large period changes in Mira variables can be associated with thermal pulses. Zijlstra & Bedding (2004) noted that a large increase in the period of BH Cru (420–540 days) was associated with changes in its spectrum, and proposed that BH Cru underwent a decrease in effective temperature not necessarily caused by a thermal pulse.

Significant period changes have not been detected for most Mira stars, a result consistent with the expectation of low rates of period change for Miras not undergoing thermal pulses. Nonetheless, smaller but still significant period changes have been identified in stars other than the eight thermal pulse candidates. Several Mira variables had non-monotonic period changes, appearing to oscillate around a mean period or around a period trend. Zijlstra & Bedding (2002) called such stars *meandering Miras*. Templeton *et al.* (2005) noted that, while the physical mechanism for period meandering was unclear, the timescales of the meandering period changes were consistent with the Kelvin–Helmholtz cooling time of the envelope (Equation 5.77). They suggested that meandering period changes might be caused by thermal relaxation oscillations in the stellar envelope, perhaps in response to the global changes caused by a thermal pulse.

Uttenthaler *et al.* (2011) searched for the short-lived radioactive element technetium in the spectra of 12 Mira variables. Its presence would be indicative of the mixing of material from deep within the star, such as might be expected during a thermal pulse. Technetium was detected in five of the stars, but Uttenthaler *et al.* found no strong correlation between the presence or absence of technetium and the type of period change observed.

8.3 Semi-Regular Variables

SR red giants, not unexpectedly (Section 3.1), have light curves that do not repeat well from cycle to cycle, but for which a persistent periodicity can nonetheless be identified. In Figure 8.9 we plot a portion of the light curve of the SRb variable Z UMa. As we saw above, SR variables are a common type of variable star. The main periods of SR variables range between tens of days and a few hundred days.

Soszyński *et al.* (2013b) identified double-mode and triple-mode SR variables in the Large Magellanic Cloud and used them to identify the pulsation modes of sequences in Figure 8.3. They found that sequences C, C′, and B were populated by brighter variables pulsating in the fundamental, first-overtone, and second-overtone radial modes, respectively. Sequence D is populated by stars with long secondary periods, which are not thought to represent any radial pulsation modes and which are discussed further below. OSARG variables were found to populate several sequences, of which sequence C′ had the longest periods. Soszyński *et al.* (2013b) also concluded that star-to-star differences in mass and metal abundance were likely responsible for the existence of broad period–luminosity sequences in

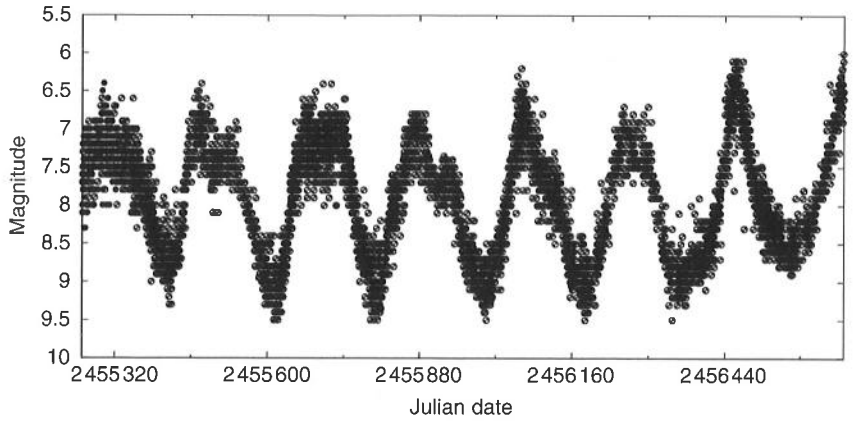

Figure 8.9 This figure shows the visual light curve of the semi-regular (SRb) variable Z UMa. (Based upon observations from the AAVSO International Database (Henden, 2013). Courtesy AAVSO.)

this diagram. As noted above, they propose the existence of a continuum between OSARG, SR, and Mira variables, with the dividing points between these groups being arbitrary. Mosser *et al.* (2013b) argued that there exists a link between the low-level solar-like oscillations observed in evolved red giants by the *Kepler* mission and the larger-amplitude variability of the OSARG variables. They proposed that the period–luminosity relations seen among OSARG variables can be seen as a continuation of the period–luminosity relations for radial modes in the red giants and asymptotic giants observed with *Kepler*.

The long secondary periods observed for some SR red giants remain a puzzle (sequence D in Figure 8.3). These secondary periods were long ago noticed by Payne-Gaposchkin (1954) and Houk (1963). They are observed for a significant number of long-period variables of both the Mira and SR types, occurring in perhaps 24–50% of such stars (Nicholls *et al.*, 2009). Nicholls *et al.* explored both binary and pulsation explanations for long secondary periods, but were unable to arrive at a satisfactory solution to the problem.

Semi-regular SRc variables are cool supergiant stars, brighter and more massive than Mira variables. Instead of having masses in the 0.6 $M_\odot$ to a few $M_\odot$ range, the SRc variables have masses around 10–20 $M_\odot$. Their MS progenitors were probably even more massive since these variables often appear to be undergoing significant mass loss. SRc variables typically have early M spectral types, indicating effective temperatures near 3000 K. The light curve of the red supergiant S Persei, an SRc variable thought to belong to the Per OB1 association, is shown in Figure 8.10.

Kiss, Szabó, & Bedding (2006) investigated the light curves of 48 red supergiant variables using data from the AAVSO International Database, finding periods ranging between about 100 and 4000 days. Multiple periods were found for several of the stars. Kiss *et al.* (2006) concluded that the shorter periods well matched those expected from pulsation in the fundamental or first-overtone

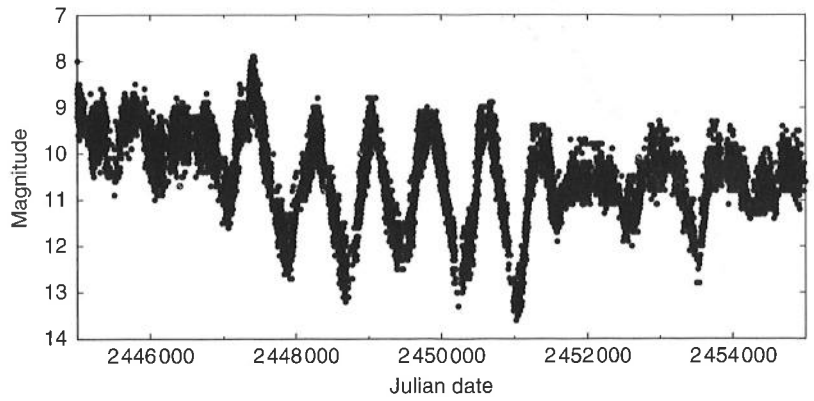

Figure 8.10 This figure shows the visual light curve of the semi-regular (SRc) variable S Persei. (Based upon observations from the AAVSO International Database (Henden, 2013). Courtesy AAVSO.)

radial modes, but that the longest periods could not be matched to either mode. They suggested that the long periods might correspond to the long secondary periods observed among SR red giant variables.

Because of the intrinsic brightness of the SRc variables (which can have $M_{\rm bol} \sim -8$), attempts have been made to see whether they obey some form of period–luminosity relation (Stothers, 1969; Pierce, Jurcevic, & Crabtree, 2000). Neglecting their longest periods, Kiss *et al.* (2006) were able to derive a period–luminosity relation of the form

$$M_K = (-3.44 \pm 0.6) \log \mathcal{P} - (1.6 \pm 1.6). \tag{8.1}$$

Betelgeuse (α Orionis), an M2Iab star, is, at 130 parsecs, one of the nearest red supergiant variables. This SRc star was one of the first stars to be successfully resolved by interferometry (Michelson & Pease, 1921), and it has subsequently been the subject of a variety of high-spatial resolution studies (Ravi *et al.*, 2011, and references therein). These observations provide evidence of extensive, non-spherically symmetric mass loss, as well as the existence of possible transient starspots on Betelgeuse's surface.

As might be expected, determination of period changes for SR variables can be more difficult than for the more regular (but still not perfectly so) Mira variables. Percy *et al.* (2008) discussed some of the problems encountered in attempting to measure period changes of red supergiant variables. A satisfactory way around these difficulties has not yet been found.

8.4 Irregular Variables

Irregular variables include, again not surprisingly (Section 3.1), those red giants and supergiants with definite variability but for which no persistent period can be

found (Lb and Lc variables, respectively). The classification of some red giants as irregular variables may, however, reflect inadequate observations. Extensive observations can sometimes be needed to discover periodicities in SR variables, and such stars can be mistakenly classified as irregular (Lebzelter, Kerschbaum, & Hron, 1995).

Lebzelter & Obbrugger (2009) investigated the light curves of 12 variables classified as SR and 12 variables classified as irregular (Lb-type). They were able to identify a period in all cases, and concluded that Lb stars formed an extension of the SR variables to shorter periods and smaller amplitudes. In their survey of variables in the Large Magellanic Cloud, Soszyński *et al.* (2009b) did not find any red giant variables with no signs of periodicity. They did, however, find SR variables that pulsated with multiple modes. Thus, it may be that all red giant variables placed within the irregular class may turn out to exhibit some periodicity when sufficient observations are available.

9
Pulsating Stars Close to the Lower Main Sequence in the H-R Diagram

In addition to solar-like pulsators, which were discussed in Section 5.11 and will not be further addressed in this chapter, Figure 3.2 reveals that four different types of pulsating stars occupy the lower MS in the H-R diagram, namely, the δ Scuti, SX Phoenicis, γ Doradus, and roAp stars. The purpose of this chapter is to discuss the properties of these stars.

Table 9.1 provides an overview of some of the main characteristics of the variable stars comprising these four classes, based on data provided, among others, by Pollard (2009), Balona *et al.* (2011a, 2012), Cohen & Sarajedini (2012), Chang *et al.* (2013), Kochukhov *et al.* (2013), Tkachenko *et al.* (2013), and the online version of the GCVS. Representative light curves are provided in Figures 9.1 (δ Scuti), 9.2 (SX Phe), 9.3 (γ Dor), and 9.4 (roAp).

9.1
δ Scuti and SX Phoenicis Stars

While the δ Sct and SX Phe nomenclature is nowadays widespread, this has not always been the case, with many different suggestions having been made previously, including, for instance, *dwarf Cepheids*, *AI Velorum stars*, *RRs stars*, and *ultra-short-period Cepheids* (see Nemec & Mateo, 1990; Breger, 1979; Gautschy & Saio, 1996; Breger, 2000, for reviews and extensive references). Perhaps the best-known (and the brightest) δ Scuti star in the sky is Altair (α Aql; Buzasi *et al.*, 2005).

As can be seen by inspection of Figure 3.2, δ Scuti and SX Phoenicis stars are both located close to an extension of the "classical" instability strip toward faint magnitudes, close to the MS locus. Accordingly, δ Scuti and SX Phoenicis stars are often bundled together as a single class. Thus, for instance, Rodríguez & Breger (2001) simply refer to SX Phe stars as one among several subgroups of "δ Scuti pulsators with non-solar surface abundances," the remaining ones being λ Boo, ρ Pup, δ Del, and classical, nonmagnetic, metallic-line Am stars (Chang *et al.*, 2013, and references therein). In general terms, δ Scuti stars are Population I stars of spectral type between about A0 and F5 (temperatures between about

Pulsating Stars, First Edition. Márcio Catelan and Horace A. Smith.